Original Article

JCBFM

Journal of Cerebral Blood Flow & Metabolism
2017, Vol. 37(3) 1095–1107

DOI: 10.1177/0271678X16650697
journals.sagepub.com/home/jcbfm
SAGE

Determination of receptor occupancy in the presence of mass dose: [^{11}C]GSK189254 PET imaging of histamine H_3 receptor occupancy by PF-03654746

Jean-Dominique Gallezot[1], Beata Planeta[1], Nabeel Nabulsi[1], Donna Palumbo[2], Xiaoxi Li[2], Jing Liu[2], Carolyn Rowinski[2], Kristin Chidsey[2], David Labaree[1], Jim Ropchan[1], Shu-Fei Lin[1], Aarti Sawant-Basak[2], Timothy J McCarthy[2], Anne W Schmidt[2], Yiyun Huang[1] and Richard E Carson[1]

Abstract

Measurements of drug occupancies using positron emission tomography (PET) can be biased if the radioligand concentration exceeds "tracer" levels. Negative bias would also arise in successive PET scans if clearance of the radioligand is slow, resulting in a carryover effect. We developed a method to (1) estimate the in vivo dissociation constant K_d of a radioligand from PET studies displaying a non-tracer carryover (NTCO) effect and (2) correct the NTCO bias in occupancy studies taking into account the plasma concentration of the radioligand and its in vivo K_d. This method was applied in a study of healthy human subjects with the histamine H_3 receptor radioligand [^{11}C]GSK189254 to measure the PK-occupancy relationship of the H_3 antagonist PF-03654746. From three test/retest studies, [^{11}C]GSK189254 K_d was estimated to be 9.5 ± 5.9 pM. Oral administration of 0.1 to 4 mg of PF-03654746 resulted in occupancy estimates of 71%–97% and 30%–93% at 3 and 24 h post-drug, respectively. NTCO correction adjusted the occupancy estimates by 0%–15%. Analysis of the relationship between corrected occupancies and PF-03654746 plasma levels indicated that PF-03654746 can fully occupy H_3 binding sites ($RO_{max} = 100\%$), and its IC_{50} was estimated to be 0.144 ± 0.010 ng/mL. The uncorrected IC_{50} was 26% higher.

Keywords

Mathematical modeling, kinetic modeling, pharmacokinetics, positron emission tomography, receptor imaging

Received 28 December 2015; Revised 8 April 2016; Accepted 13 April 2016

Introduction

Positron emission tomography (PET) studies are ideally performed using tracer doses of radioligand that occupy a negligible fraction of the targeted receptors, in order to obtain unbiased binding parameters and reduce the variability of the results. When the affinity of the radioligand for the target receptors is high or when the bioavailability of the radioligand is high, then only a very small mass of radioligand can be injected in order to achieve negligible occupancy. On the other hand, a sufficient amount of radioactivity should be injected in order to obtain low-noise images or time-activity curves (TACs) for analysis. These two constraints may not be compatible depending on the specific activity (SA) that can be achieved during

[1]Yale PET Center, Yale University, New Haven, CT, USA
[2]Pfizer Worldwide Research and Development, Cambridge, MA, USA

Corresponding author:
Jean-Dominique Gallezot, Positron Emission Tomography (PET) Center, Yale University, 801 Howard Avenue, PO Box 208048, New Haven, CT 06520-8048, USA.
Email: jean-dominique.gallezot@yale.edu

the radiosynthesis, and a higher level of radioligand occupancy might be needed in these cases. Examples of radioligands which are or were routinely injected at non-tracer (NT) dose levels include the dopamine D2/D3 radioligands [^{11}C]-(+)-PHNO[1,2] and [^{11}C]FLB 457.[3] These NT dose conditions lead to the underestimation of binding parameters such as the volume of distribution V_T[4] or the binding potential BP_{ND},[4] poorer test/retest reliability, increased inter-subject variability, or erroneous results derived of these parameters if the injected mass of radioligand is not consistent across studies or groups. Another phenomenon that can occur in the NT dose condition is the so called carryover (CO) effect, in which the results of a subsequent scan are influenced by the injected mass of a previous scan, if the two scans are performed close to each other in time, and the radioligand clearance from the plasma and/or organ of interest is slow, i.e., a non-negligible concentration of unlabeled radioligand from the first injection is still present by the time of the second injection. This leads to further underestimation and variability of the binding parameters in the second scan.

When PET studies are performed to study the in vivo properties of a drug in development, these combined non-tracer carryover (NTCO) effects on the PET parameters induce biases on the final estimated drug properties, such as errors in the plasma concentration needed to achieve 50% occupancy (IC_{50}) or on the maximal amount of receptor occupancy (RO) that the drug can achieve (RO_{max}).

In this study, we present a method to correct for NTCO effects. This involves (1) estimation of the in vivo K_d of a radioligand from test–retest studies for radioligand exhibiting NTCO effects and (2) correction for the radioligand occupancy of the targeted receptor in drug occupancy studies. This method was applied to a human RO study with 6-[(3-cyclobutyl-2,3,4,5-tetrahydro-1*H*-3-benzazepin-7-yl)oxy]-*N*-[^{11}C]methyl-3-pyridinecarboxamide hydrochloride ([^{11}C]GSK189254), a histamine H_3 receptor antagonist[5,6] with high affinity in vivo in humans (11 pM) and slow clearance from the plasma in part due to slow metabolism.[7] These correction algorithms were used to determine the IC_{50} of the H_3 antagonist study drug (1*R*,3*R*)-*N*-ethyl-3-fluoro-3-[3-fluoro-4-(pyrrolidin-1-ylmethyl)phenyl]cyclobutane-1-carboxamide (PF-03654746).[8,9] Histamine H_3 receptors are G-protein-coupled presynaptic autoreceptors that regulate cyclic AMP and inhibits the release of histamine,[10] thus antagonists such as PF-03654746 should increase synaptic histamine levels. Histamine H_3 receptors are also presynaptic heteroreceptors that modulate the release of other neurotransmitters.[11] Histamine H_3 antagonists have been investigated as promising targets to treat metabolic disorders and neurological or psychiatric disorders.[12]

Material and methods

Correction of occupancy estimates

Theory. Usually, PET studies are performed with the radiopharmaceutical administered at "tracer" mass dose, which is typically defined as less than 5%–10% occupancy of the target by the radioligand.[4] Target occupancy studies are performed with PET scans initiated after the administration of pharmacological doses of a competitive drug. Here, we consider cases where the PET studies are performed with significant mass dose, so that there is some RO by the radioligand. Suppose we make measurements of the binding potential BP_{ND} during several baseline or post-drug studies (A, B, C...), such that

$$BP_{ND}^{A} = BP_{ND}\left(1 - r^{A}\right) \tag{1}$$

where r^A is the RO during scan A due to *all* sources (endogenous, radioligand, and test drug) and BP_{ND} refers to the binding potential in the absence of all competitors. Let L be the (free) mass concentration of radioligand (nM), D be the mass concentration of test drug (nM), and N be the concentration of endogenous neurotransmitter (nM). Then, under equilibrium conditions, the total occupancy of the receptor for scan A is

$$r^{A} = 1 - \frac{1}{1 + \frac{L^{A}}{K_d^{L}} + \frac{D^{A}}{K_d^{D}} + \frac{N^{A}}{K_d^{N}}} \tag{2}$$

where the superscript on K_d refers to the radioligand, drug, or neurotransmitter. Denote the normalized concentration, $\delta_L^A = L^A/K_d^L$, the ratio of mass concentration of the radioligand to its K_d (and use similar notations δ_D^A and δ_N^A for the drug and neurotransmitter, respectively)

$$r^{A} = 1 - \frac{1}{1 + \delta_L^A + \delta_D^A + \delta_N^A} = \frac{\delta_L^A + \delta_D^A + \delta_N^A}{1 + \delta_L^A + \delta_D^A + \delta_N^A} \tag{3}$$

Note that in the definition of δ_L^A and δ_D^A, the concentrations and K_d values could be replaced by plasma levels and IC_{50} values, or by drug/radioligand mass doses and ED_{50} values. One simplification of equation (3) is worth noting. First in the case of no competing neurotransmitter ($\delta_N^A = 0$) and under true "tracer" dose condition ($\delta_L^A = 0$)

$$r^{A} = 1 - \frac{1}{1 + \delta_D^A} = \frac{\delta_D^A}{1 + \delta_D^A} \tag{4}$$

which is the conventional occupancy relationship. Similarly, if a radioligand is used at a NT dose, its self-occupancy, in the absence of drug and neurotransmitter, denoted r_L^A, is equal to $\delta_L^A/(1+\delta_L^A)$.

Suppose two studies, A and B, are performed with different drug (D) levels. Then

$$BP_{ND}^B = BP_{ND}(1-r^B) \tag{5}$$

The apparent drug occupancy of study B with respect to study A ($r^{A,B}$) is usually computed as follow

$$r^{A,B} = 1 - \frac{BP_{ND}^B}{BP_{ND}^A} \tag{6}$$

If study A is performed at tracer levels, i.e., $BP_{ND}^A = BP_{ND}$, then $r^{A,B} = r^B$. If not, then

$$r^{A,B} = 1 - \frac{1-r^B}{1-r^A} = \frac{r^B - r^A}{1-r^A} \tag{7}$$

Now, consider the case of study A with no drug, study B with drug, and ignore the effects of neurotransmitters, but not the effect of the radioligand mass dose. Then, the measured occupancy, $r^{A,B}$ is

$$r^{A,B} = \frac{\delta_D^B + \delta_L^B - \delta_L^A}{1+\delta_D^B+\delta_L^B} \tag{8}$$

It is straightforward to see that equation (8) reduces to the form of equation (4) in the absence of a mass dose effect with the radioligand ($\delta_L^A = \delta_L^B = 0$). Our goal is to calculate the RO that would have occurred in the absence of tracer mass effect (i.e., r^B) from the measured value $r^{A,B}$. Rearranging equation (4) yields

$$\delta_D^B = \frac{r^B}{1-r^B} \tag{9}$$

and plugging equation (9) into equation (8) yields

$$r^{A,B} = \frac{r^B + (\delta_L^B - \delta_L^A)(1-r^B)}{1+\delta_L^B(1-r^B)} \tag{10}$$

Solving for r^B yields

$$r^B = \frac{r^{A,B}(1+\delta_L^B) + \delta_L^A - \delta_L^B}{1+\delta_L^A - \delta_L^B + r^{A,B}\delta_L^B} \tag{11}$$

Equation (11) is the formula for converting the apparent occupancy, $r^{A,B}$, to the true occupancy in the absence of radioligand mass effect, r^B.

Occupancy plot

When binding potentials BP_{ND} cannot be estimated directly, due to the lack of a reference region, the occupancy plot[13] is often used, under the assumptions that the occupancy and non-displaceable volume of distribution V_{ND} are the same across all regions. For baseline and blocking studies (A and B), the occupancy plot is a plot of $V_T^A - V_T^B$ as a function of V_T^A, and the slope and x-intercept of the regression line correspond to the occupancy r^B and V_{ND}, respectively, under tracer mass dose conditions. When tracer mass dose conditions are not met, then V_T^A and V_T^B are

$$\begin{aligned} V_T^A &= V_{ND} + BP_{ND}(1-r^A) \\ V_T^B &= V_{ND} + BP_{ND}(1-r^B) \end{aligned} \tag{12}$$

And thus

$$\begin{aligned} V_T^A - V_T^B &= BP_{ND}(1-r^A) - BP_{ND}(1-r^B) \\ &= BP_{ND}(r^B - r^A) \\ BP_{ND} &= \frac{V_T^A - V_{ND}}{1-r^A} \end{aligned}$$

And finally

$$V_T^A - V_T^B = (V_T^A - V_{ND})\frac{(r^B - r^A)}{(1-r^A)} = (V_T^A - V_{ND})r^{A,B} \tag{13}$$

Equation (13) shows that the occupancy plot under NT mass dose conditions can be used to estimate V_{ND} and $r^{A,B}$, for use in equation (11), in the same manner that apparent occupancy $r^{A,B}$ is computed from BP_{ND} estimates for radioligands that have a reference region.

Please also note that equation (13) is a generalization of equation (6) in Cunningham et al.[13]: indeed, if the radioligand was injected at tracer mass dose, but drug was present during both scans A and B (with doses D^A and D^B, respectively) then $r^B = D^B/(D^B + IC_{50})$ and $r^A = D^A/(D^A + IC_{50})$, and equation (13) can then be rearranged to match equation (6) in Cunningham et al.[13]

Implementation of the correction. In order to use equation (11) to estimate "true" drug occupancy, knowledge of δ_L^A and δ_L^B is required, which reflect the ratio of the ligand concentration (L) to the K_d of the radioligand. If PET scans are performed at equilibrium then the equilibrium free plasma level could be used. For bolus injections, we will assume that the appropriate ligand concentration is the mass concentration (in pM) in plasma averaged between two time-points t_1 and t_2,

and multiplied by the plasma free fraction (f_P). After fitting the plasma ligand mass data from times t_1 to t_2 to one exponential, i.e., $L^A(0)e^{-\alpha^A t}$, the ligand mass concentration L^A to be attributed to scan A is

$$L^A = \frac{L^A(0)}{\alpha^A(t_2 - t_1)}\left(e^{-\alpha^A t_1} - e^{-\alpha^A t_2}\right) \quad (14)$$

For studies B (second study) and C (third study), the ligand mass concentrations, L^B and L^C, taking into account the residual (CO) ligand mass from the previous injection(s) are

$$L^B = \frac{L^B(0)}{\alpha^B(t_2 - t_1)}\left(e^{-\alpha^B t_1} - e^{-\alpha^B t_2}\right) + L^A e^{-\alpha^A \Delta t^{A,B}} \quad (15)$$

$$L^C = \frac{L^C(0)}{\alpha^C(t_2 - t_1)}\left(e^{-\alpha^C t_1} - e^{-\alpha^C t_2}\right) + L^A e^{-\alpha^A \Delta t^{A,C}} + L^B e^{-\alpha^B \Delta t^{B,C}} \quad (16)$$

where $\Delta t^{A,B}$, $\Delta t^{A,C}$, and $\Delta t^{B,C}$ are the differences in injection times between studies A and B, A and C, and B and C, respectively

Determination of K_d^L from test–retest data. If no previous estimate of the in vivo K_d^L is available, then in order to use equation (11) in a real occupancy study, the value of K_d^L can be estimated from the test–retest study data, in cases where the presence of ligand mass dose results in a detectable apparent occupancy when comparing the test and retest scans. To do this, consider equation (10) for the test–retest study with no drug on board (i.e., $\delta_D^B = 0$)

$$r^{T,R} = \frac{\delta_L^R - \delta_L^T}{1 + \delta_L^R} = \frac{L^R - L^T}{K_d^L + L^R} \quad (17)$$

where the superscripts T and R designate the test and retest studies, respectively. Solving for K_d^L yields

$$K_d^L = \frac{L^R - L^T}{r^{T,R}} - L^R \quad (18)$$

Thus, from the test–retest studies, calculate the ligand mass doses, L^T and L^R, (equations (14) and (15)) and the apparent occupancy $r^{T,R}$, and use equation (18) to determine K_d^L. Ideally, these values will be consistent across multiple test–retest studies. Based on results from all test–retest studies, determine the average K_d^L and use that value for the occupancy studies in the calculation of δ_L^A and δ_L^B values and the application of equation (11). Equation (18) is analogous to equation (5) in Madsen et al.,[14] which estimated ID_{50} from test/retest scans, based on differing mass doses of ligand.

Study plan

The proposed method was used to quantify the occupancy at the histamine H_3 receptor by PF-03654746[8,9] using the radioligand [^{11}C]GSK189254.[6] Nine male subjects were included in this study (age = 35 ± 10 years, range = 21–48 years; body weight = 81 ± 6 kg, range = 73–90 kg). The study was conducted in compliance with the ethical principles originating in or derived from the Declaration of Helsinki and in compliance with all International Conference on Harmonization Good Clinical Practice guidelines. In addition, all local regulatory requirements were followed, in particular, those affording greater protection to the safety of trial participants. These studies were performed under protocols approved by the Yale School of Medicine Human Investigation Committee, the Yale-New Haven Hospital Radiation Safety Committee, and the Yale University Radiation Safety Committee. Subjects were recruited by public advertisement. Written informed consent was obtained from all participants after full explanation of study procedures.

A total of 24 scans were performed in this study. Three subjects participated in the test–retest study, and six subjects participated in the drug occupancy study. For the test–retest study, subjects were scanned twice with [^{11}C]GSK189254 on the same day, 3.4 ± 0.1 h apart. For the occupancy study, subjects were scanned three times with [^{11}C]GSK189254: two times on the same day, 5.4 ± 0.12 h apart, and one time on the next day, 25.9 ± 0.8 h after the first scan. The study drug PF-03654746 (0.1, 0.25, 0.5 (two subjects), 1.5, or 4 mg) was administered immediately after the baseline scan, and the second and third PET scans were performed at ~3 h and ~24 h post-dosing.

Radiochemistry

[^{11}C]GSK189254 was radiolabeled with [^{11}C]methyl iodide by slight modification of the original reported method,[6] thru *N*-alkylation of the precursor's carbamoyl group, either in solution using the FXC synthesis module (GE Medical Systems) or via the Captive Solvent method[15] using the AutoLoop synthesis module. Briefly, [^{11}C]methyl iodide was swept with helium through the FXC reactor vessel cooled to 0°C which contained a solution of the precursor (1 mg) and potassium hydroxide (3 N KOH; 3 µL) in 150 µL dimethylformamide (DMF) until radioactivity peaked, and the resulting mixture was then heated for 5 min at 80°C. Alternatively, [^{11}C]methyl iodide was swept with helium through the stainless steel loop preloaded with a

solution of the precursor (0.5–0.6 mg) in 80 μL of DMF containing KOH (1 N; 1.6–2 μL), and the resulting mixture was allowed to stand for 5 min at ambient temperature.

The crude product resulting from both methods was purified by reverse-phase high-performance liquid chromatography (HPLC). The HPLC product fraction was further purified by solid-phase extraction, and then formulated in saline containing less than 10% ethanol. The PET drug product solution was finally passed through a 0.22 micron membrane filter for terminal sterilization and collected in a sterile vial, affording a sterile formulated I.V. solution ready for dispensing and administration. The average radiochemical and chemical purity ($n = 24$) was $99.8\% \pm 0.1\%$ and $98.4\% \pm 5.6\%$, respectively. The SA at the end of synthesis was 245 ± 166 MBq/nmol.

PET and magnetic resonance imaging data acquisition

PET studies were performed on the HR+ scanner (Siemens/CTI, Knoxville, TN, USA). Dynamic data were acquired in 3D mode for 2 h following the injection of 281 ± 173 MBq of [^{11}C]GSK189254 by a computer-controlled infusion pump (Harvard PHD 22/2000, Harvard Apparatus, Holliston, MA, USA). The radioligand SA at time of injection (TOI) was 110 ± 80 MBq/nmol. The injected mass was 13 ± 6 ng/kg (max 22 ng/kg). Dynamic data were binned into 33 frames (6×0.5 min, 3×1 min, 2×2 min, 22×5 min) and reconstructed with the Ordered Subset Expectation Maximization algorithm including corrections for attenuation, normalization, scatter, randoms, and deadtime. Image voxel size was $2.06 \times 2.06 \times 2.42$ mm.

Each subject also underwent a brain MR scan on a 3T Trio (Siemens Medical Systems, Erlangen, Germany) with a circularly polarized head coil. MR acquisition was a Sag 3D magnetization-prepared rapid gradient-echo sequence with 3.34 ms echo time, 2500 ms repetition time, 1100 ms inversion time, 7° flip angle, and 180 Hz/pixel bandwidth. The image dimensions were $256 \times 256 \times 176$, and pixel size was $0.98 \times 0.98 \times 1.0$ mm.

Arterial input function measurements

Whole blood and plasma. Both continuous and sequential discrete arterial blood samples were taken as previously described.[16]

Determination of ligand metabolism in plasma. The arterial plasma samples collected after injection at 3, 8, 15, 30, 60, and 90 min for the test–retest study, and at 8, 30, 60, 75, and 90 min for occupancy study, were analyzed using HPLC and the column-switching method[17] to measure the unchanged fraction of [^{11}C]GSK189254. See supplemental data for details.

Plasma free fraction. The plasma free fraction f_P of [^{11}C]GSK189254 was measured by ultrafiltration as previously described.[16]

Scaled arterial input function. In the drug occupancy study, for four out of the six studies performed 24 h post-drug administration, arterial blood data were not available. For these studies, the arterial input function obtained during the baseline scan was scaled, taking into account the difference in injected dose, and used to apply in the kinetic model.

Fit of the tail of the arterial input function. In order to compute the [^{11}C]GSK189254 in vivo K_d value and the corrections in the occupancy study, the tail of the arterial input function (last five points) was fitted to a single exponential function, using non-linear-weighted least squares. The weights were computed to take into account the counting statistics in the plasma sample radioactivity measurements.

Kinetic modeling

Motion correction. The PET dynamic images were motion corrected after reconstruction: an early summed image (0–10 min post-injection) was created as reference, then each frame image was smoothed using a Gaussian filter with a full width at half maximum of 3 mm, then a rigid coregistration matrix was estimated between the reference image and the smoothed frame images, using a mutual information algorithm (FLIRT, FSL 3.2, Analysis Group, FMRIB, Oxford, UK), and finally the original (unsmoothed) frame images were resliced to match the reference image.

Computation of regional TACs. Regions-of-interest (ROIs) were taken from the Anatomical Automatic Labeling template.[18] Eleven gray matter ROIs were selected: cerebellum (84 cm^3), amygdala (3.7 cm^3), caudate (16 cm^3), putamen (17 cm^3), thalamus (17 cm^3), hippocampus (15 cm^3), insula (29 cm^3), the anterior cingulate (22 cm^3), frontal (256 cm^3), occipital (81 cm^3), and parietal (65 cm^3) cortices. One extra white matter ROI (37 cm^3) was manually drawn on the template magnetic resonance image (MRI) in the centrum semiovale. To apply these ROIs to the PET data, two coregistration matrices were computed, first between the template MRI and each subject's MRI (using a 12-paramter affine transform), and then between each subject's MRI and each PET early summed image (using a

six-parameter rigid transform) using a mutual information algorithm (FLIRT, FSL 3.2, Analysis Group, FMRIB, Oxford, UK).

Kinetic analysis. Regional volumes of distribution (V_T) for [^{11}C]GSK189254 were computed using the two-tissue compartment (2TC) model (for review see Gunn et al.[19]) with the parameters k_4 and K_1/k_2 shared across all regions ($2TC_{shared}$), as in previous studies.[7] For test–retest studies, the test–retest variability (TRV) of V_T estimates was computed as $2 \times \left(V_T^R - V_T^T\right)/\left(V_T^R + V_T^T\right)$. The one-tissue compartment (1TC) model, the (unconstrained) 2TC model, and the multilinear analysis MA1[20] (with $t^* = 30$ min) were also evaluated.

PK of PF-03654746

A total of four venous blood samples per subject were drawn to measure PF-03654746 plasma concentration (PK) during the PET scans. Blood was drawn at the beginning and end of each post-dose PET scan, i.e. at approximately 3, 5, 24, and 26 h after drug administration. Samples were assayed using HPLC tandem mass spectrometric method (HPLC-MS/MS), with a lower limit of quantification of 0.025 ng/mL. To obtain a single PK value per scan, the geometric mean of the two PK measurements obtained at the beginning, and end of each scan was determined.

Results

Arterial input function data

The parent fraction of [^{11}C]GSK189254 in arterial plasma was high during the entire PET scan, with $93\% \pm 3.9\%$ ($n = 16$) of radioactivity in plasma attributed to unchanged [^{11}C]GSK189254 at 60 min post-injection.

The plasma free fraction was $50\% \pm 3.0\%$ ($n = 24$). There was no significant difference between test ($49\% \pm 1.6\%$, $n = 3$) and retest ($47\% \pm 1.9\%$, $n = 3$) studies (Paired Student t-test, $p = 0.51$). In the occupancy study, plasma free fraction tended to be slightly lower in post-drug studies ($49\% \pm 3.6\%$ at 3 h, $51\% \pm 1.9\%$ at 24 h, $n = 6$) than at baseline ($53\% \pm 2.6\%$, $n = 6$), but the difference was not significant when correcting for multiple comparisons (Paired Student t-test, $p = 0.07$).

The tails of the metabolite-corrected plasma curve were fitted to perform the self-occupancy correction. These fits were performed assuming either a single exponential decay rate for all studies or differing decay rates for individual scans. A common exponential clearance rate α was sufficient to describe all available arterial input function curves ($n = 20$) according to the F-test ($F_{19,60} = 0.71$ and $p = 0.80$). Thus, for each subject, in equations (12) to (14), all α values could be assumed to be identical. α was estimated to be 0.14 ± 0.02 per h, i.e., a 5-h half-life. The plasma clearance (dose/AUC of plasma) was 0.59 ± 0.07 (L/kg/h) ($n = 20$).

For test studies, the average metabolite-corrected plasma concentration L^T at the end of the scans was 7.2 ± 0.5 pM ($n = 3$), and in retest studies, the concentration L^R, accounting for the CO mass effect, was higher: 11.4 ± 1.3 pM ($n = 3$). In the occupancy studies, the concentration L^A was 6.0 ± 2.3 pM ($n = 6$), and the corrected concentrations, L^B and L^C, were 6.3 ± 1.9 pM and 4.3 ± 1.3 pM, respectively ($n = 6$).

[^{11}C]GSK189254 kinetic analysis

The kinetics of [^{11}C]GSK189254 can often be described well by the 1TC model, but not for all ROIs and subjects. Comparing the 2TC and 1TC model fits using the F-test, the 2TC model provided significantly better fits in only 91 out of 288 fits ($F_{2,29} > 3.33$, $p < 0.05$, uncorrected for multiple tests). No ROIs were always fitted better by the 2TC model. However, when the 2TC model was used, outlier V_T estimates were observed 54 times out of 288 fits (i.e., values higher than the regional median plus five times the regional median absolute deviation from the nine test or baseline scans). Using a constrained version of the 2TC model (i.e., $2TC_{shared}$) removed the outliers. MA1 and $2TC_{shared}$ V_T estimates were very well correlated (the regression line equation was $y = 0.976x + 0.546$, $r^2 = 0.989$, with the $2TC_{shared}$ V_T used as the independent variable). Thus, MA1 could be also used to quantify [^{11}C]GSK189254 V_T values. However, the $2TC_{shared}$ results were used for the occupancy computations, since this was the model selected in previous studies.[7]

TRV of [^{11}C]GSK189254 V_T estimates

Supplementary Figure S1 shows, for one representative subject, the [^{11}C]GSK189254 concentration images acquired from 60 to 90 min post-injection under the test and retest conditions. The average V_T estimates ranged from 9.4 ± 2.3 mL/cm^3 ($n = 3$) in the centrum semiovale to 47 ± 6.7 mL/cm^3 ($n = 3$) in the putamen (Table 1). The average relative standard error of V_T estimated from the model fits was $\leq 10\%$ in all regions. The inter-subject coefficient of variation of V_T values ranged from 3% in the hippocampus to 25% in the central semiovale.

The retest V_T values were generally lower than the test V_T values in all regions: the TRV ranged from $-11\% \pm 8.6\%$ in the cerebellum ($n = 3$) to $-26\% \pm 15\%$ in the caudate ($n = 3$).

Table 1. [^{11}C]GSK189254 V_T estimates from test scans and test retest variability ($n = 3$).

	Test V_T			TRV	
	Mean	%SD	%SE	Mean	SD
Putamen	47	14	5.0	−23	11
Caudate	37	16	6.8	−26	15
Anterior cingulate	28	8.4	4.5	−18	5.7
Insula	24	9.3	3.4	−19	5.6
Amygdala	23	13	5.6	−19	8.3
Thalamus	18	12	3.4	−14	6.3
Frontal cortex	16	10	3.5	−16	5.5
Parietal cortex	14	2.8	2.9	−16	5.0
Hippocampus	14	2.6	3.4	−12	6.6
Occipital cortex	12	1.2	2.8	−16	4.3
Cerebellum	12	10	2.9	−11	8.6
Central semiovale	9.4	25	7.1	−13	16

TRV: test–retest variability: $2 \times (V_T^{Retest} - V_T^{Test})/(V_T^{Retest} + V_T^{Test})$.

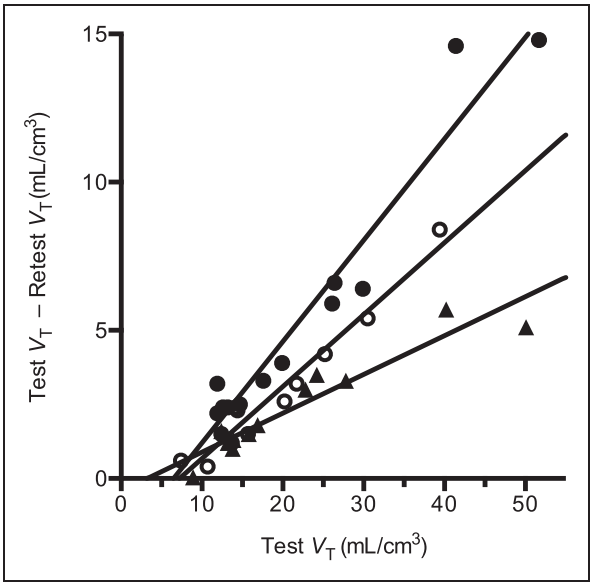

Figure 1. Occupancy plots for test/retest [^{11}C]GSK189254 studies for subjects 1 to 3 (solid circles, solid triangles, and open circles, respectively).

[^{11}C]GSK189254 in vivo K_d estimates

The self-occupancy plots for all three test–retest studies are shown in Figure 1. Based on these occupancy plots, the apparent self-occupancy values were 34%, 13%, and 24% for the three test–retest studies. The non-displaceable distribution volume (V_{ND}) was estimated to be 5.6 ± 2.2 mL/cm^3 (mean ± SD, $n = 3$). Using equation (18), the in vivo K_d of [^{11}C]GSK189254 was estimated to be 9.5 ± 5.9 pM (mean ± SEM, $n = 3$).

Occupancy study

There were no serious adverse events following the administration of PF-03654746. In one subject, following the administration of 0.5 mg of PF-03654746, the following adverse events were observed: anxiety, parasomnia, night sweats, nausea, headache, and hypoaesthesia.

Figure 2 shows [^{11}C]GSK189254 concentration images acquired from 60 to 90 min post-injection from the baseline and two post-drug scans for one subject in the occupancy study. Substantial reduction in specific binding was evident at 3 h post-dose, and partial recovery of H_3 availability was observed at 24 h. The average regional [^{11}C]GSK189254 V_T estimates under baseline and post-drug conditions are listed in Table 2. In this second cohort, the baseline V_T ranged from 11 ± 2.1 mL/cm^3 in the centrum semiovale to 46 ± 9.3 mL/cm^3 in the putamen ($n = 6$). At 3-h post-drug, V_T values ranged from 4.8 ± 0.60 mL/cm^3 in the centrum semiovale to 12 ± 6.4 mL/cm^3 in the putamen. At 24-h post-drug, V_T values ranged from 7.0 ± 1.6 mL/cm^3 in the centrum semiovale to 22 ± 12 mL/cm^3 in the putamen.

A sample occupancy plot from one subject in the occupancy study is shown in Figure 3. The apparent occupancies estimated from all occupancy plots are listed in Table 3. Apparent occupancies ranged from 30% to 95%. After correcting for self-occupancy from the CO mass (equation (11), Table 3), occupancies ranged from 30% to 97%, with CO mass effect correction ranging from 0% to +15%.

The relationship between PK of PF-03654746 and estimated RO is shown in Figure 4 with their fits to the simple occupancy model, either assuming 100% maximum occupancy, or allowing it to float as a second parameter (RO_{max}). With the self-occupancy correction, the RO_{max} was not significantly different from 100% ($F_{1,10} = 0.16$, $p = 0.70$; $RO_{max} = 99\% \pm 2\%$), and the IC_{50} from the one-parameter fit was 0.144 ± 0.010 ng/mL (0.447 nM). Without self-occupancy correction, RO_{max} was significantly lower than 100% ($F_{1,10} = 6.3$, $p < 0.05$): RO_{max} was $95\% \pm 2\%$ and IC_{50} was 0.182 ± 0.0184 ng/mL, which was 26% higher than the corrected value. When RO_{max} is fixed to 100% in fitting the PK versus uncorrected occupancy values relationship, the impact of the NTCO effect on the IC_{50} is larger: with RO_{max} set to 100%, the uncorrected IC_{50} was estimated to 0.22 ± 0.02 ng/mL, which is 53% higher than the corrected value.

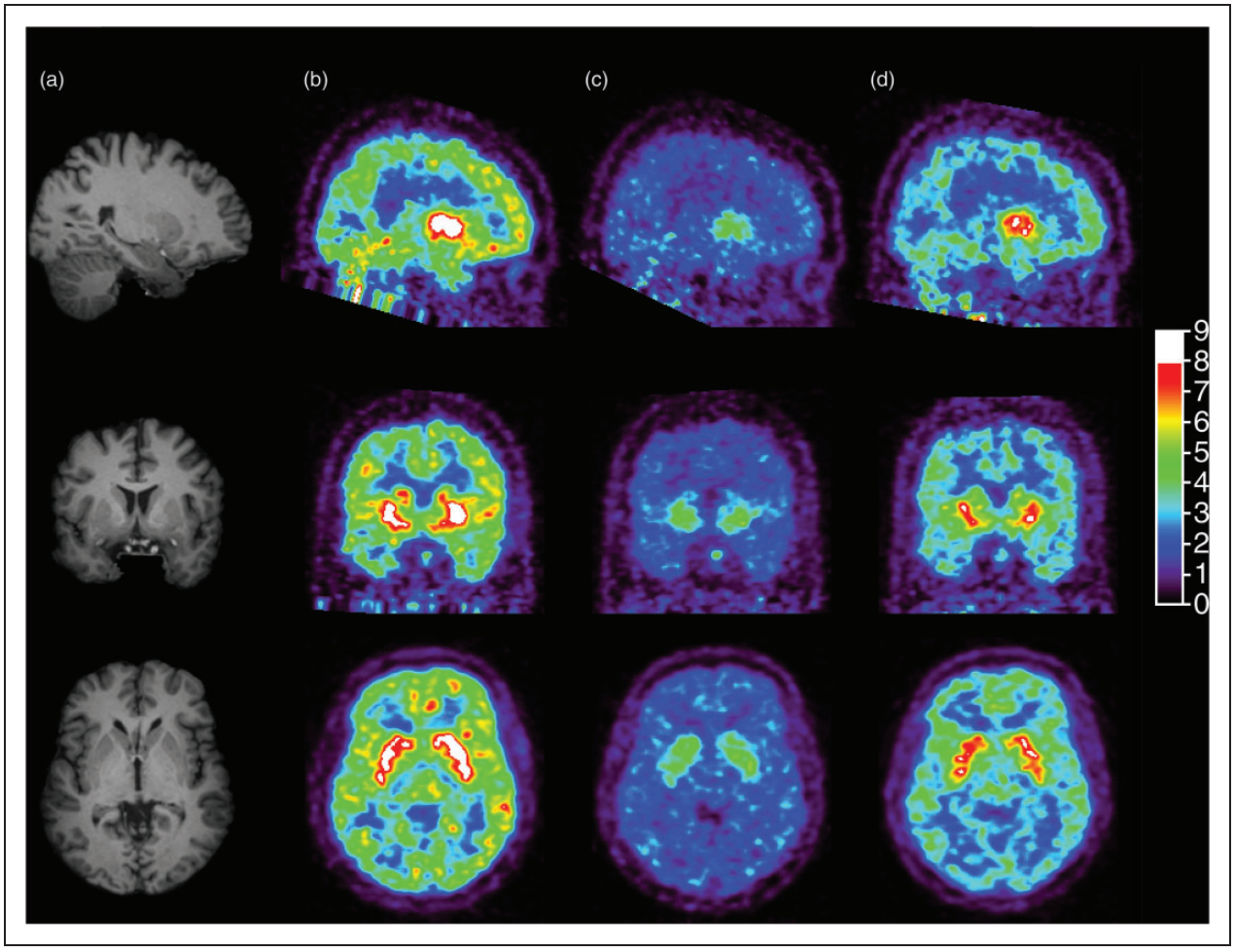

Figure 2. Sagittal (top), coronal (middle) and transverse (bottom) MR images (a) and brain images of [^{11}C]GSK189254 standard uptake value at 60–90 min post-injection during the baseline scan (b), the 3-h post-drug scan (c) and the 24-h post-drug scan (d) for a representative subject who received a dose of 0.5 mg of PF-03654746.

Table 2. [^{11}C]GSK189254 V_T estimates from drug occupancy studies.

	Baseline ($n = 6$)		3 h post-drug administration[a] ($n = 6$)		24 h post-drug 2administration[a] ($n = 6$)	
	Mean	SD	Mean	SD	Mean	SD
Putamen	46	9.3	12	6.4	22	12
Caudate	32	4.7	8.5	3.5	15	7.1
Anterior cingulate	29	4.8	8.7	3.6	14	6.3
Insula	25	4.2	8.1	2.9	13	5.5
Amygdala	24	5.1	7.6	2.8	12	5.1
Thalamus	18	2.0	7.2	2.1	10	3.0
Frontal cortex	18	2.2	6.3	2.0	9.6	3.5
Parietal cortex	16	2.0	6.1	1.8	8.9	3.0
Hippocampus	14	1.9	6.2	1.4	8.5	2.0
Occipital cortex	15	2.3	6.1	1.7	8.7	2.7
Cerebellum	14	0.40	5.7	1.4	8.3	2.0
Central semiovale	11	2.1	4.8	0.60	7.0	1.6

[a]Post-drug values are average across all doses of PF-03654746: 0.1, 0.25, 0.5 (two subjects), 1.5, or 4 mg.

Discussion

We have developed and implemented a method for correction for NTCO effects in PET receptor studies. This method is applicable for radioligands with high affinity, high bioavailability, and slow plasma clearance, so that RO is non-negligible. The need for this approach can be found in test/retest data with reductions in binding measures in retest scans caused by CO effects. We have applied this technique to the H_3 antagonist radioligand [^{11}C]GSK189254 and used it to measure the occupancy and in vivo IC_{50} of PF-03654746.

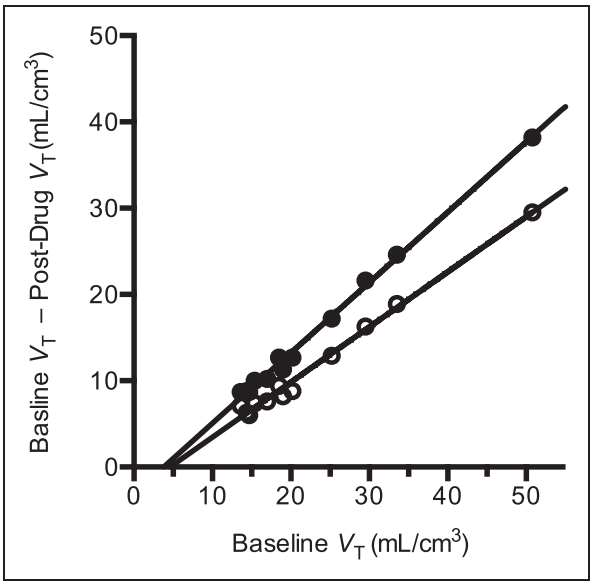

Figure 3. Sample occupancy plots from a PF-03654746 occupancy study (0.5 mg), at 3-h post-drug (solid circles) and at 24-h post-drug (open circles). The occupancies estimated from the slope of these regression lines were 82% ± 2% and 64% ± 2% at 3 h and 24 h after drug, respectively. The non-displaceable volumes of distribution estimated from the *x*-intercept of these regression lines were 3.8 ± 0.5 mL/cm^3 and 4.6 ± 0.7 mL/cm^3 at 3 h and 24 h after drug, respectively.

The properties of the H_3 radioligand [^{11}C]GSK189254 in humans and its kinetic modeling were previously reported,[7] and our results had similarities and differences from these reports. The high unchanged fraction of [^{11}C]GSK189254 measured in this study is consistent with previous literature reports. In this study, the unchanged fraction was 93% ± 3.9% at 60 min post-injection, while in a previous study, it was 86% ± 5% at 75 min post-injection.[7] The plasma free fraction measure in this study was somewhat higher that in the aforementioned previous study: 50% ± 3% instead of 36%.[7] Interestingly, there was more difference between the two studies concerning the order of magnitude of [^{11}C]GSK189254 volumes of distribution in the brain, even though the same compartmental model was used for data analysis. In this study, baseline V_T values ranged from 9.4 mL/cm^3 in the central semiovale (12 mL/cm^3 in cerebellum) to 47 mL/cm^3 in the putamen. In the previous study, baseline V_T values were about twofold higher, ranging from 22.5 mL/cm^3 in the cerebellum to 119 mL/cm^3 in the putamen. The value of [^{11}C]GSK189254 in vivo K_d in humans found in this study, 9.5 pM, is close to the value found in a previous self-saturation study using unlabeled GSK189254: the EC_{50} in humans had been estimated to be 11 pM.[7]

The in vivo K_d estimated here was determined from the reduction in V_T between test and retest scans due to CO effects. Since the studies were not performed at

Table 3. [^{11}C]GSK189254 apparent and corrected occupancies of PF-03654746.

Subject	PF-03654746 (mg)	Time since drug administration (h)	Uncorrected *RO* (%)	Corrected *RO* (%)[a]	Difference[b]
1	0.5	3	82	89	7
		24	64	77	13
2	4.	3	95	97	2
		24	90	93	4
3	1.5	3	92	96	4
		24	77	88	11
4	0.25	3	74	80	5
		24	52	61	9
5	0.5	3	85	91	6
		24	59	75	15
6	0.1	3	66	71	5
		24	30	30	0

RO: receptor occupancy. [a]Corrected RO based on equation (11). [b]The difference between uncorrected and corrected RO values is expressed in percentage points.

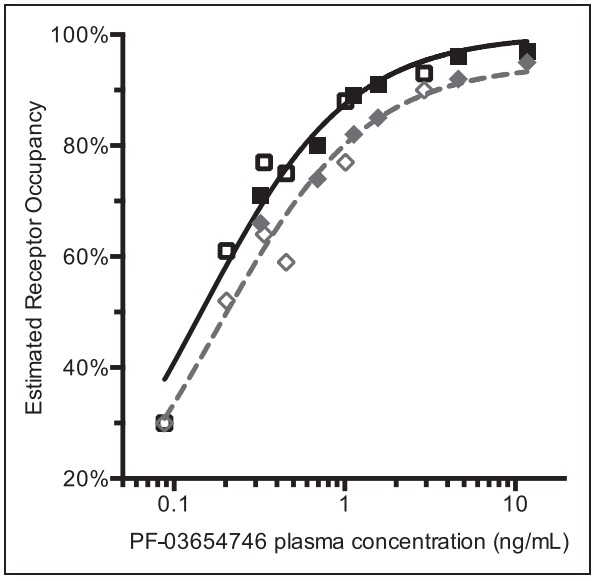

Figure 4. PF-03654746 receptor occupancy vs. PK relationship using uncorrected occupancy estimates (in gray diamonds) and using corrected occupancy estimates (in black squares). Solid symbols represent 3-h post-drug data; open symbols represent 24-h post-drug data. The dashed gray line represents the best apparent RO-PK fit, using the two-parameter occupancy model (RO_{max} and IC_{50}), and the solid black line represents the best corrected RO-PK fit, using the one-parameter occupancy model (IC_{50}). Without correction for the radioligand occupancy, RO_{max} was estimated to be lower than 100%, but after correction, RO_{max} was no longer statistically different from 100%.

equilibrium from the radioligand point of view (i.e., bolus injections were used), the plasma concentration of the radioligand was changing over time. Thus, the plasma concentrations used in all computations, and in particular in the computation of the radioligand in vivo K_d, are dependent on the choice of the time interval t_1:t_2 (equations (14) and (15)). However, this effect is likely to be small, since this NTCO correction is, by definition, suited for radioligands with plasma concentration that do not decrease rapidly. For [^{11}C]GSK189254, the difference between plasma levels between 15 and 60 min and between 60 and 120 min was only $9\% \pm 6\%$ ($n = 20$).

The choice of the time interval t_1:t_2 can have a stronger effect on the estimation of the rate of decrease α of the plasma concentration, and then the extrapolation of the radioligand plasma concentration used in the correction of the CO effect. This may have a potentially larger effect on the accuracy of the correction, and this extrapolation is challenging to validate since it is difficult to measure accurately the concentration of radioligand remaining in the plasma at the time of post-drug PET scans (at ~5 h or ~26 h after the baseline injection). In this study, using the 15–60 min time interval instead of 60–120 min changed the estimate of the parameter α from 0.14 ± 0.019 to 0.22 ± 0.038 per h; this, in turn changed the estimates of [^{11}C]GSK189254 in vivo K_d from 9.5 ± 5.9 pM to 7.3 ± 4.9 pM, (see Supplementary Table 1). This effect had a minor impact on the PF-03654746 IC_{50}, changing it from 0.144 ± 0.010 ng/mL to 0.128 ± 0.010 ng/mL. Assessing whether multi-exponential fits would be less sensitive to the selection of the time interval was not possible, since we could not reliably estimate two washout rates except for the 15–120 min time interval. With a bi-exponential fit over a 15–120-min time interval, the slowest washout rate was estimated to be 0.056 ± 0.016 per h, i.e., a slower washout than that estimated with any mono-exponential fit. This would lead to a larger K_d value (17 ± 14 pM, instead of 9.5 ± 5.9 pM) and to a slightly larger IC_{50} (0.176 ± 0.011 ng/mL, instead of 0.144 ± 0.010 ng/mL).

The plasma free fraction f_P of [^{11}C]GSK189254 was very stable between scans, and f_P was in a range of values (~50%) which provides highly reliable data. This is a very favorable property of [^{11}C]GSK189254 when using the plasma concentration to correct for the NTCO effect. However, for other tracers with very low plasma free fraction, f_P estimates tend not to be robust, and may not be useful in the plasma concentration computation. Ignoring f_P would lead to a bias in the tracer K_d estimate, i.e., only K_d/f_P can be estimated. However, if the plasma free fraction is biologically stable across scans, it should be possible to use the total (i.e., free + bound) plasma concentration when applying the NTCO correction. If the tracer plasma free fraction is both low and variable, V_T estimates are expected to be variable; this may hide the NTCO effect in test and retest paradigms and lead to noisier occupancy estimates in drug occupancy studies.

This NTCO correction is suitable for radioligands that are both used at NT dose levels and have a CO effect. For radioligands that are used at NT dose levels, but with sufficiently fast plasma clearance so that no CO effect is detectable, equations (1) to (14) remain valid and can be used for correcting occupancy estimates; however, it would be necessary to perform a study where the mass of radioligand is varied[7,14,21] in order to estimate the radioligand in vivo K_d value. In particular, as mentioned above, a controlled saturation study was previously performed to evaluate [^{11}C]GSK189254 in vivo K_d value in humans,[7] and the K_d value of the present study (9.5 pM) is very similar to that of the saturation study (11 pM).

In this study, all apparent occupancies $r^{A,B}$ were positive values and always lower than the true occupancy r^B. However, the apparent occupancies are not

guaranteed to be in the [0, r^B] interval. First, based on equation (10), it can be shown that $r^{A,B} < r^B$, if and only if

$$\delta_L^B < \delta_L^A/(1 - r^B) = \delta_L^A(1 + \delta_D^B)$$

Thus, as expected, a sufficient condition for the apparent occupancy to be lower than the true occupancy is for the radioligand's mass concentration during the post-drug scan to be less than that during the baseline scan. However, if the radioligand's concentration after drug administration is greater than the radioligand's concentration at baseline multiplied by the factor $1 + \delta_D^B$, then the apparent occupancy will be higher than the true occupancy. Thus, a CO effect, or a low-specific activity/high-radioligand mass during the post-drug scan is needed to observe apparent occupancies higher than the true occupancy. The presence of the factor $1/(1 - r^B)$ in the above equation also shows that the apparent occupancy is less likely to overestimate the true occupancy for high-drug occupancy conditions than for low-drug occupancy conditions. Since in this study the true drug occupancy was always relatively high (estimated $r^B \geq 30\%$), the observed $r^{A,B}$ values were always lower than the corrected r^B values.

Based on equation (8), depending on the normalized concentrations of radioligand and drug, the apparent occupancy will be positive if and only if

$$\delta_L^A < \delta_L^B + \delta_D^B$$

Thus, the apparent occupancy will be positive when the radioligand's normalized concentration at baseline is lower than the sum of the radioligand and drug normalized concentrations during the post-drug scan. Thus, a low-specific activity/high-radioligand mass during the baseline scan, combined with little or no CO effect, is needed to observe negative apparent occupancies.

If all scans were performed with the same normalized radioligand concentration (i.e., $\delta_L^B = \delta_L^A$, thus no CO), then the apparent radioligand occupancy will underestimate the true occupancy by a factor $1 - r_L^B$, where r_L^B is the radioligand self-occupancy in the absence of drug (i.e., $(\delta_L^B/(1 + \delta_L^B))$), at low-drug doses, and will reach the true occupancy at high-drug doses. For relatively moderate radioligand self-occupancies ($r_L^B \leq 50\%$), the maximal difference between r^B and $r^{A,B}$ is proportional to r_L^B, e.g., reaching 17 percentage points when r_L^B is 50%. The ultimate goal of a RO study is often to estimate the drug's RO_{max} and IC_{50}. Since all the equations used in the present NTCO correction assume equilibrium conditions for both the radioligand and drug, assuming that all scans were performed with the same normalized radioligand concentration (i.e., $\delta_L^B = \delta_L^A$, thus no CO), the errors in RO_{max} and IC_{50} when using $r^{A,B}$ instead of r^B are the errors that one would expect from a classical in vitro binding assay. Specifically, RO_{max} is unbiased but the measured IC_{50} using $r^{A,B}$ ($\widehat{IC_{50}}$) overestimates the true IC_{50} by a factor equal to $1 + \delta_L^B$ (i.e., $\widehat{IC_{50}} = IC_{50}(1 + \delta_L^B)$). This is analogous to the relationship between IC_{50} and K_i (i.e., $IC_{50} = K_i(1 + \delta_L)$) in an in vitro binding assay.[22] Additional discussion of the quantitative impact of the carry over of radioligand mass is available in the supplemental data file, in particular in supplementary Figures 2 to 4.

If possible, it is desirable to perform all scans of an occupancy study using a constant injected mass of radioligand (in μg or in μg/kg of body weight), since the bias and the correction of the apparent occupancy values will be (more) consistent across subjects if the self-occupancy and CO effects are comparable. However, this may not always be achievable if the specific activity of the radioligand is variable, or if the radioligand plasma kinetics varies from scan to scan (i.e., even with a constant injected mass, the plasma concentration is variable). Applying a correction taking into account the variability of the ligand concentration across scans is therefore useful to make best use of all scan data.

This correction could be useful for other tracers with very high affinity for their target. For example, [^{11}C]-(+)-PHNO has high affinity in vitro and in vivo for dopamine D_3 receptors,[1,23] and NTCO effects are possible in D_3 rich regions such as the substantia nigra as indicated by test–retest studies.[24] More importantly using [^{11}C]-(+)-PHNO, there is a particular interest to evaluate the selectivity of drugs for the dopamine D_2 and D_3 receptors,[25] and thus accurately measuring a drug's IC_{50} for both receptors in vivo is particularly important. The present correction algorithm could be used for [^{11}C]-(+)-PHNO in regions with ~100% D_3 binding, such as the substantia nigra; however, the algorithm must be extended in order to be applied to brain regions with a mixed D_2 and D_3 signal, such as the globus pallidus.

Conclusion

In this study, a method was introduced to correct drug occupancy studies for NTs dose of radioligand and CO effects from one scan to the next. The method was applied to a study of H_3 occupancy, based on changes in baseline binding observed in test/retest studies. This correction method can be useful to improve RO measurements and to reduce biases and variability of the estimates of drug IC_{50} and maximal occupancy.

Funding

The author(s) disclosed receipt of the following financial support for the research, authorship, and/or publication of this article: Yale-Pfizer Bioimaging Alliance; CTSA Grant UL1 RR024139 from the National Center for Research Resources (NCRR) and the National Center for Advancing Translational Sciences (NCATS) components of the National Institutes of Health (NIH).

Acknowledgments

The authors appreciate the excellent technical assistance of the staff at the Yale University PET Center and the Pfizer New Haven CRU. The authors would also like to acknowledge Helene Faessel and Bob Williams for helpful discussions. This study was supported by the Yale-Pfizer Bioimaging Alliance. This publication was also made possible by CTSA Grant UL1 RR024139 jointly from the National Center for Research Resources (NCRR) and the National Center for Advancing Translational Sciences (NCATS) components of the National Institutes of Health (NIH). Its contents are solely the responsibility of the authors and do not necessarily represent the official view of NIH.

Declaration of conflicting interests

The author(s) declared the following potential conflicts of interest with respect to the research, authorship, and/or publication of this article: DP, XL, JL, CR, KC, ASB, TJM, and AWS were employees of Pfizer at the time of this research. YH declares significant financial interest in Pfizer, Inc. The remaining authors declare no conflict of interest.

Authors' contributions

JDG and BP contributed to analysis and interpretation of data. NN, DL, and JR contributed to ligand radiosynthesis and acquisition of data. SFL contributed to metabolite analysis and acquisition of data. CR and KC contributed to medical coordination and study planning. ASB and AWS contributed to conception and design and translational pharmacology/biology. DP contributed to conception and design and interpretation of data. XL contributed to interpretation of data and statistical analysis. JL contributed to PK analysis and interpretation of data. TJM, YH, and REC contributed to study concept and design, study coordination, analysis, and interpretation of data. JDG, BP, SFL, NN, and REC drafted the manuscript. All co-authors revised the manuscript.

Supplementary material

Supplementary material for this paper can be found at http://jcbfm.sagepub.com/content/by/supplemental-data

References

1. Gallezot J-D, Beaver JD, Gunn RN, et al. Affinity and selectivity of [^{11}C]-(+)-PHNO for the D3 and D2 receptors in the rhesus monkey brain in vivo. *Synapse* 2012; 66: 489–500.
2. Searle GE, Beaver JD, Tziortzi A, et al. Mathematical modelling of [^{11}C]-(+)-PHNO human competition studies. *Neuroimage* 2013; 68: 119–132.
3. Olsson H, Halldin C and Farde L. Differentiation of extrastriatal dopamine D2 receptor density and affinity in the human brain using PET. *Neuroimage* 2004; 22: 794–803.
4. Innis RB, Cunningham VJ, Delforge J, et al. Consensus nomenclature for in vivo imaging of reversibly binding radioligands. *J Cereb Blood Flow Metab* 2007; 27: 1533–1539.
5. Medhurst AD, Atkins AR, Beresford IJ, et al. GSK189254, a novel H3 receptor antagonist that binds to histamine H3 receptors in Alzheimer's disease brain and improves cognitive performance in preclinical models. *J Pharmacol Exp Ther* 2007; 321: 1032–1045.
6. Plisson C, Gunn RN, Cunningham VJ, et al. ^{11}C-GSK189254: a selective radioligand for in vivo central nervous system imaging of histamine H3 receptors by PET. *J Nucl Med* 2009; 50: 2064–2072.
7. Ashworth S, Rabiner EA, Gunn RN, et al. Evaluation of 11C-GSK189254 as a novel radioligand for the H3 receptor in humans using PET. *J Nucl Med* 2010; 51: 1021–1029.
8. Brioni JD, Esbenshade TA, Garrison TR, et al. Discovery of histamine H3 antagonists for the treatment of cognitive disorders and Alzheimer's disease. *J Pharmacol Exp Ther* 2010; 336: 38–46.
9. Wager TT, Pettersen BA, Schmidt AW, et al. Discovery of two clinical histamine H3 receptor antagonists: trans-N-ethyl-3-fluoro-3-[3-fluoro-4-(pyrrolidinylmethyl)phenyl] cyclobutanecarboxamide (PF-03654746) and trans-3-fluoro-3-[3-fluoro-4-(pyrrolidin-1-ylmethyl)phenyl]- N-(2-methylpropyl)cyclobutanecarboxamide (PF-03654764). *J Med Chem* 2011; 54: 7602–7620.
10. Arrang JM, Garbarg M and Schwartz JC. Auto-inhibition of brain histamine release mediated by a novel class (H3) of histamine receptor. *Nature* 1983; 302: 832–837.
11. Leurs R, Blandina P, Tedford C, et al. Therapeutic potential of histamine H3 receptor agonists and antagonists. *Trends Pharmacol Sci* 1998; 19: 177–183.
12. Esbenshade TA, Fox GB and Cowart MD. Histamine H3 receptor antagonists: preclinical promise for treating obesity and cognitive disorders. *Mol Interv* 2006; 6: 77–88, 59.
13. Cunningham VJ, Rabiner EA, Slifstein M, et al. Measuring drug occupancy in the absence of a reference region: the Lassen plot re-visited. *J Cereb Blood Flow Metab* 2010; 30: 46–50.
14. Madsen K, Marner L, Haahr M, et al. Mass dose effects and in vivo affinity in brain PET receptor studies–a study of cerebral 5-HT4 receptor binding with [11C]SB207145. *Nucl Med Biol* 2011; 38: 1085–1091.
15. Wilson AA, Garcia A, Jin L, et al. Radiotracer synthesis from [(11)C]-iodomethane: a remarkably simple captive solvent method. *Nucl Med Biol* 2000; 27: 529–532.
16. Gallezot J-D, Nabulsi N, Neumeister A, et al. Kinetic modeling of the serotonin 5-HT(1B) receptor radioligand [(11)C]P943 in humans. *J Cereb Blood Flow Metab* 2010; 30: 196–210.

17. Hilton J, Yokoi F, Dannals RF, et al. Column-switching HPLC for the analysis of plasma in PET imaging studies. *Nucl Med Biol* 2000; 27: 627–630.
18. Tzourio-Mazoyer N, Landeau B, Papathanassiou D, et al. Automated anatomical labeling of activations in SPM using a macroscopic anatomical parcellation of the MNI MRI single-subject brain. *Neuroimage* 2002; 15: 273–289.
19. Gunn RN, Gunn SR and Cunningham VJ. Positron emission tomography compartmental models. *J Cereb Blood Flow Metab* 2001; 21: 635–652.
20. Ichise M, Toyama H, Innis RB, et al. Strategies to improve neuroreceptor parameter estimation by linear regression analysis. *J Cereb Blood Flow Metab* 2002; 22: 1271–1281.
21. Delforge J, Loc'h C, Hantraye P, et al. Kinetic analysis of central [76Br]bromolisuride binding to dopamine D2 receptors studied by PET. *J Cereb Blood Flow Metab* 1991; 11: 914–925.
22. Cheng Y and Prusoff W. Relationship between the inhibition constant (K1) and the concentration of inhibitor which causes 50 per cent inhibition (I50) of an enzymatic reaction. *Biochem Pharmacol* 1973; 22: 3099–3108.
23. Freedman SB, Patel S, Marwood R, et al. Expression and pharmacological characterization of the human D3 dopamine receptor. *J Pharmacol Exp Ther* 1994; 268: 417–426.
24. Gallezot J-D, Zheng M-Q, Lim K, et al. Parametric imaging and test-retest variability of 11C-(+)-PHNO binding to D2/D3 dopamine receptors in humans on the high-resolution research tomograph PET scanner. *J Nucl Med* 2014; 55: 960–966.
25. Day M, Bain E, Marek G, et al. D3 receptor target engagement in humans with ABT-925 using [11C](+)-PHNO PET. *Int J Neuropsychopharmacol* 2010; 13: 291–292.